JSR Publications

Available Online

J. Sci. Res. **18** (1), 91-106 (2026)

JOURNAL OF SCIENTIFIC RESEARCH

www.banglajol.info/index.php/JSR

Accelerating Bianchi I Universe with Time Varying Deceleration Parameter in *f(G)* Gravity

M. S. Palaspagar[1*], P. P. Khade[2], P. R. Patil[2]

[1]Department of Mathematics, Rajarshee Shahu Science College, Chandur Rly District, Amravati 444904, India

[2]Department of Mathematics, Vidya Bharati Mahavidyalaya, Camp Amravati 444601, India

Received 1 June 2025, accepted in final revised form 8 October 2025

Abstract

The present research aims at investigating the LRS Bianchi type I dark energy cosmological model within the framework of $f(G)$ gravity. To obtain solutions for the field equations, a parametrization of the deceleration parameter is employed. The approximate best-fit values of the model parameters are obtained using the least squares method, incorporating observational constraints from available datasets such as the Hubble dataset and the Pantheon dataset by applying the Root Mean Square Error (RMSE) formula. The related cosmological parameters are graphed against redshift, and the universe's accelerated expansion is subsequently examined. Various physical parameters, including pressure, energy density, and energy conditions, are also discussed.

Keywords: LRS Bianchi type-I space-time; *f(G)* Gravity; Cosmic string; Statefinder diagnostics; Observational constraints.

doi: https://dx.doi.org/10.3329/jsr.v18i1.81946 J. Sci. Res. **18** (1), 91-106 (2026)

1. Introduction

A viable physical theory must meet three essential standards: internal consistency, comprehensive explanatory power, and empirical validation through experimental evidence. This trio of criteria equally applies to gravitational theories, including General Relativity. Despite its successes, the theory is marred by singularities like black holes and the Big Bang, and it fails to align with observational evidence at infrared scales [1]. Relativistic astrophysicists have proposed modified gravity theories by generalizing the Einstein-Hilbert action. This involves substituting the Ricci scalar with more complex functions, such as $f(R)$, or combining scalar and tensorial curvature invariants. This approach has become a standard framework for exploring the underlying causes of the universe's accelerated expansion. This modification gives rise to the $f(R)$ theory of gravitation [2]. Another extension of gravitational theory is $f(G)$, which incorporates the

*Corresponding author: mamta.palaspagar@rssc.edu.in

Gauss-Bonnet curvature invariant G. This framework enables the development of consistent models that satisfy local General Relativity constraints. Notably, the invariant G can eliminate ghost contributions and aid in regularizing the gravitational action.

In recent years, numerous cosmological models have been developed within the framework of $f(G)$ theory, accommodating various physical fluids. Researchers have employed diverse approaches, including the Noether symmetry method, to explore $f(G)$ cosmology. Studies have also focused on cosmological solutions in the context of specific models, such as the ΛCDM model, and have investigated the coupling of four-dimensional spacetimes with Gauss-Bonnet gravity, as suggested by [3-5]. Furthermore, bouncing cosmology and static spherically symmetric star solutions have been explored within the $f(G)$ gravity framework [6-8]. Additionally, string bulk viscous cosmological models have been examined in the context of $f(G)$ theory [9].

Bianchi Universes serve as valuable tools for analyzing cosmological models characterized by anisotropic and homogeneous backgrounds. Their pedagogical significance stems from their ability to model homogeneous yet anisotropic universes. Recent observations [10-15], such as those from WMAP, suggest that the standard cosmological model requires modification to accommodate anisotropic features, echoing the morphology of Bianchi Universes. Furthermore, evidence indicates that the universe was not initially smooth, particularly during the inflationary period, and may have retained some degree of inhomogeneity.

Fayaz *et al.* [16] derived precise power-law solutions for anisotropic universes within the framework of Gauss-Bonnet gravity. Li *et al*. [17] probed the universe's late-time acceleration. Meanwhile, *Nojiri et al.* [18] introduced a novel concept: Gauss-Bonnet dark energy. Moreover, it was shown that there are some viable $f(G)$ models that can pass the solar system test [19,20]. Shekh *et al*. [21] discussed Quintessential $f(G)$ gravity with a statistical fitting of $H(z)$. A theoretical framework where the gravitational action incorporates functions of the Gauss-Bonnet invariant has also been explored in the literature for its potential to replicate cosmic evolution [21-38].

Recent studies have explored a variety of cosmological models in both general relativity and modified theories of gravity. For instance, tilted two-fluid cosmological models with variable G and Λ have been investigated within the framework of general relativity [39]. Models based on the $f(R,T)$ theory have also been developed, where cosmologies filled with a perfect fluid source were analyzed in detail [40]. In addition, magnetized dark energy cosmological models with a time-dependent cosmological term have been considered in the context of Lyra geometry [41]. Quark and strange quark matter in the $f(R,T)$ theory of gravity have been constrained using observational data [42], while two-fluid cosmological models in $f(T)$ gravity have been tested against observations to explore their viability [43]. Two interacting fluids with quadratic EOS in a five-dimensional Bianchi model were proposed [44], while higher-dimensional spherically symmetric string cosmological models with a zero-mass scalar field in Lyra geometry have been considered [45].

In the present study, the Bianchi Type-I universe is investigated within the framework of $f(G)$ gravity, utilizing the deceleration parameter $q = b - \frac{n}{H}$, as previously proposed by [46,47]. This strategy is employed to fine-tune the model and determine the best-fit values of the parameters b and n. Through comparative analysis of theoretical predictions and observational data, the optimal parameter set that aligns with empirical evidence is identified using statistical methods. The analysis is based on observational Hubble data (OHD) samples, providing a robust framework for testing the cosmological model against a broad spectrum of observational constraints.

The paper is strutrured as follows: Section 2 presents a concise overview of $f(G)$ gravity and its mathematical formulation. Section 3 provides deterministic solutions of the field equations with varying deceleration parameters. To restrict the model parameters, Section 4 employs observational Hubble datasets. Section 5 is devoted to apparent magnitude and luminosity distance. Section 6 discusses cosmographic parameters and energy conditions. Finally, Section 7 summarizes the findings and outlines their broader implications.

2. Overview and Mathematical Formulation of $f(G)$ Gravity

The action of the $f(G)$ gravity is given by

$$S = \frac{1}{2K}\int [R + f(G)]\sqrt{-g}d^4x + S_\varphi(g_{ij}, \varphi) \quad (1)$$

where, g_{ij} is the metric tensor, S_φ is the action of matter. The matter is minimally coupled to the metric tensor g_{ij} which means that $f(G)$ is a purely metric theory of gravity. The scalar field φ represents the matter fields. Thus, the action depends on both the metric and the matter fields.

The function *f(G)* is an arbitrary function of the Gauss-Bonnet invariant *G*, defined as

$$G = R^2 - 4R_{ij}R^{ij} + R_{ij\mu\nu}R^{ij\mu\nu} \quad (2)$$

where, R is the Ricci scalar, R_{ij} stands for Ricci tensor and $R_{ij\mu\nu}$ denotes Riemannian tensors.

By varying the action (1) with respect to the metric gij, we obtain the field equations

$$R_{ij} - \frac{1}{2}Rg_{ij} + \delta\left[R_{i\mu jv} + R_{\mu j}g_{vi} - R_{\mu v}g_{ji} - R_{ij}g_{v\mu} + R_{iv}g_{j\mu} + \frac{1}{2}R\left(R_{ij}g_{\mu v} - g_{iv}g_{j\mu}\right)\right]\nabla^\mu\nabla^v + (Gf_G - f)g_{ij} = kT_{ij} \quad (3)$$

Here ∇^μ denotes the covariant derivative and $f(G)$ stand for the derivative of $f(G)$ with respect to G.

The Friedmann-Robertson-Walker (FRW) metric accurately describes the present universe, but it is unlikely that the universe's geometry remained isotropic throughout its evolution. In the early universe, anisotropy is more plausible. Bianchi models generalize FRW spacetimes and allow for anisotropic expansion.

Here, we consider the LRS Bianchi type-I metric:

$$ds^2 = dt^2 - A^2dx^2 - B^2(dy^2 + dz^2), \quad (4)$$

The Bianchi type I model, characterized by metric potentials A and B that vary with cosmic time t, offers a more comprehensive framework than the isotropic FRW models. This model is particularly significant in describing the universe's early evolution, as it

provides a homogeneous representation with flat spatial sections. Although the spatial geometry is flat, the expansion dynamics can be anisotropic.

The Ricci scalar R and Gauss-Bonnet (GB) invariant for Bianchi type I is found to be

$$R = -2\left[\frac{\ddot{A}}{A} + 2\frac{\ddot{B}}{B} + 2\frac{\dot{A}\dot{B}}{AB} + \frac{\dot{B}^2}{B^2}\right] \tag{5}$$

$$G = 8\left[\frac{\ddot{A}\dot{B}^2}{AB^2} + 2\frac{\dot{A}\dot{B}\ddot{B}}{AB^2}\right] \tag{6}$$

where the dot $(\dot{})$ denotes differentiation with respect to cosmic time t.

According to Grand Unified Theories (GUTs), after the universe cooled below a critical temperature, spontaneous symmetry breaking occurred, producing stable topological defects. One-dimensional defects are called cosmic strings, which are believed to play a role in galaxy formation.

For anisotropic fluids, we assume the following energy–momentum tensor:

$$T_v^{\mu} = diag[\rho,\ -p_x, -p_y, -p_z], \tag{7}$$

where, ρ is the energy density of the fluid, and p_x, p_y, p_z are the pressures along x, y, z axes, respectively.

The anisotropic fluid is characterized by the equation of state (EoS) given as

$$p = \omega\rho, \tag{8}$$

where, ω need not be constant.

From (7), the tensor can be expressed as

$$T_v^{\mu} = diag[1,\ -\omega_x, -\omega_y, -\omega_z]\rho, \tag{9}$$

where, $\omega_x, \omega_y, \omega_z$ are the directional EoS parameters along the $x, y, and\ z$ axes; ω is a deviation-free EoS parameter of the fluid.

To parametrize deviations from isotropy, set $\omega_x = \omega$, and the skewness parameter δ is introduced to describe deviations from ω along the $y\ and\ z$ directions.

Thus, in this case, the energy–momentum tensor is expressed as

$$T_v^{\mu} = diag[1,\ -\omega, -(\omega+\delta), -(\omega+\delta)]\rho, \tag{10}$$

The mean Hubble parameter is

$$H = \frac{1}{3}(H_1 + 2H_2), \tag{11}$$

where, $H_1 = \frac{\dot{A}}{A}$, $H_2 = H_3 = \frac{\dot{B}}{B}$, are the directional Hubble parameter's.

The expansion scalar θ, shear scalar σ are defined as

$$\theta = u^i_{;i} = \frac{\dot{A}}{A} + 2\frac{\dot{B}}{B}, \tag{12}$$

$$\sigma = \sigma_{\mu v}\sigma^{\mu v} = \frac{1}{\sqrt{3}}\left(\frac{\dot{A}}{A} - \frac{\dot{B}}{B}\right). \tag{13}$$

The average scale factor a is defined via the proper volume:

$$V = a^3 = AB^2. \tag{14}$$

Finally, substituting the metric (4) into the field equations (3), we obtain the independent equations of motion:

$$\frac{\dot{B}^2}{B^2} + 2\frac{\ddot{B}}{B} - 16\frac{\ddot{B}\dot{B}}{B^2}\dot{f}_G - 8\frac{\dot{B}^2}{B^2}\ddot{f}_G + Gf_G - f = -k\omega\rho \tag{15}$$

$$\frac{\ddot{A}}{A} + \frac{\ddot{B}}{B} + \frac{\dot{A}\dot{B}}{AB} - 8\left(\frac{\ddot{A}\dot{B}}{AB} + \frac{\dot{A}\ddot{B}}{AB}\right)\dot{f}_G - 8\frac{\dot{A}\dot{B}}{AB}\ddot{f}_G + Gf_G - f = -k(\omega+\delta)\rho \tag{16}$$

$$\frac{\dot{B}^2}{B^2} + 2\frac{\dot{A}\dot{B}}{AB} - 24\frac{\dot{A}\dot{B}^2}{AB^2}\dot{f}_G + Gf_G - f = k\rho \tag{17}$$

3. Solution of the Field Equations with Varying Deceleration Parameter

Here, three equations (15–17) involving six parameters: $A, B, p, \rho,$ and f, are presented. To construct a physically viable and observationally consistent cosmological model, the following assumptions are made.

(i) Form of $f(G)$

A power-law form of the Gauss–Bonnet function is considered:

$$f(G) = \beta G^m, \tag{18}$$

where, β and m are arbitrary constants.

(ii) Relation between directional Hubble Parameters

We employ a linear relation between the directional Hubble parameters H_1 and H_2:

$$H_1 = \alpha H_2, \tag{19}$$

where, $\alpha \geq 0$ is a constant controlling the anisotropy of the model. This choice leads to a proportionality between the shear scalar σ and the expansion scalar θ, i.e., $\sigma \propto \theta$.

(iii) Time-varying deceleration parameter

A time-dependent deceleration parameter of the form is assumed:

$$q = b - \frac{n}{H} \tag{20}$$

where, b, n are constants.

The Hubble parameter H and the deceleration parameter q serve as essential tools for understanding cosmic evolution within various cosmological frameworks. The Hubble parameter provides insight into the current expansion rate of the universe, while the deceleration parameter characterizes its acceleration status, distinguishing between accelerating ($q < 0$) and decelerating ($q > 0$) phases. This transition is strongly supported by recent astrophysical evidence, including observations of Type Ia supernovae [41,42] and cosmic microwave background (CMB) anisotropies [43]. Within the framework of $f(G)$ gravity, this formulation is particularly useful, as it captures key dynamical features of cosmic evolution without requiring a complex equation of state. These derivations help reveal the dynamical effects of $f(G)$ gravity and further clarify whether the model can reproduce the observed cosmic acceleration or even predict novel behavior unique to the $f(G)$ framework.

In general, the deceleration parameter is defined as

$$q = \frac{d}{dt}\left(\frac{1}{H}\right) - 1 \tag{21}$$

By comparing equations (19) and (20), and choosing

$$c = -\frac{(b+1)}{n}$$

A point-type singularity is encountered at $t = 0$.

The Hubble parameter and the scale factor then take the forms

$$H = \frac{n\, e^{nt}}{(b+1)(e^{nt}-1)} \tag{22}$$

$$a = \eta(e^{nt} - 1)^{\frac{1}{(b+1)}}, \tag{23}$$

where, $\eta = \delta(b+1)^{\frac{1}{(b+1)}}$.

3.1. *The deceleration parameter $q(t)$ in terms of cosmic time*

From equs. (20) and (21), the deceleration parameter in terms of cosmic time is

$$q = -1 + \frac{(b+1)}{e^{nt}} \tag{24}$$

In our model, when

$$t = \frac{1}{n}\log\left[\eta(1+z)^{-(b+1)} + 1\right],$$

the sign of q changes.

This gives a relation between cosmic time t, redshift z, and the scale factor

$$a(t) = (1+z)^{-1}.$$

The Hubble parameter (H) in terms of redshift (z) is

$$H = \frac{n}{b+1}\left[\eta(1+z)^{(b+1)} + 1\right], \tag{25}$$

Finally, the Hubble rate function takes the form

$$H = \frac{H_0}{1+\eta}\left[\eta(1+z)^{(b+1)} + 1\right], \tag{26}$$

where $H_0 = 100h$ is the Hubble constant at $z = 0$, and η, b are free parameters to be estimated by observations.

3.2. *Transformation rule*

To relate cosmic time and redshift, we use

$$H(z) = -\frac{1}{1+z}\frac{dz}{dt} \tag{27}$$

Thus, the deceleration parameter in terms of z becomes

$$q = \frac{b(1+z)^{(b+1)}) - \eta}{(1+z)^{(b+1)} + \eta} \tag{28}$$

3.3. *Evolution of H*

Using equation (25) and

$$\dot{H} = \frac{dH}{dt}, \tag{29}$$

and $\dot{H} = -(1+z)H(z)\frac{dH}{dz}$ (30)

we obtain

$$\dot{H} = -\frac{\eta(b+1)H_0^2}{(1+\eta)^2}(1+z)^{(b+1)}[\eta(1+z)^{(b+1)} + 1]. \tag{31}$$

3.4. *Energy density and pressure*

Substituting H and $\dot{H}$, the energy density and pressures are

$$\rho = \frac{9(1+2\alpha)H_0^2}{k(\alpha+2)^2(1+\eta)^2}[\eta(1+z)^{(b+1)}+1]^2 \quad (32)$$

3.5. *Directional pressures*

$$p_x = \frac{6n^2}{k\eta^2(\alpha+2)(b+1)}\left[(1+z)^{2(b+1)}+\eta(1+z)^{(b+1)}\right] - \frac{27\,H_0^2}{k(\alpha+2)^2(1+\eta)^2}\left[\eta(1+z)^{(b+1)}+1\right]^2 \quad (33)$$

$$p_y = p_z = \frac{3n^2(\alpha+1)}{k\eta^2(\alpha+2)(b+1)}\left[(1+z)^{2(b+1)}+\eta(1+z)^{(b+1)}\right]$$

$$-\frac{9H_0^2(\alpha^2+\alpha+1)}{k(\alpha+2)^2(1+\eta)^2}[\eta(1+z)^{(b+1)}+1]^2 \quad (34)$$

The expansion scalar and the shear scalar turn out to be

$$\theta = \frac{3H_0}{(1+\eta)}[\eta(1+z)^{(b+1)}+1] \quad (35)$$

$$\sigma = \frac{\sqrt{3}(\alpha-1)}{(\alpha+2)}\frac{H_0}{1+\eta}[(\eta(1+z)^{b+1}+1)] \quad (36)$$

The evolution of the shear $\sigma(z)$ indicates that the shear magnitude $|\sigma(z)|$ increases monotonically with redshift for both parameter choices $\alpha = 1.001$ and $\alpha = 1.1$. Importantly, the dimensionless ratio $|\sigma/H|$, which directly measures the anisotropy relative to the Hubble expansion, also grows with redshift and remains significant around the recombination epoch (zrec≈1100z). This behavior demonstrates that shear does not decay at high redshift; instead, it persists and even amplifies as $z \to \infty$.

The Deceleration Parameter becomes as

$$q = \frac{b(1+z)^{(b+1)})-\eta}{(1+z)^{(b+1)}+\eta} \quad (37)$$

The EoS and Skewness parameter turn out to be

$$\omega = \frac{-3}{(1+2\alpha)} + \frac{2(\alpha+2)n^2(1+\eta)^2(1+z)^{(b+1)}}{3\eta^2(b+1)(1+2\alpha)H_0^2}\frac{[(1+z)^{(b+1)}+\eta]}{[\eta(1+z)^{(b+1)}+1]^2} \quad (38)$$

$$\delta = \frac{(2-\alpha-\alpha^2)}{(1+2\alpha)}\left\{1 - \frac{n^2(1+\eta)^2(1+z)^{(b+1)}}{3(b+1)\eta^2H_0^2}\frac{[(1+z)^{(b+1)}+\eta\,]}{[\eta(1+z)^{(b+1)}+1]^2}\right\} \quad (39)$$

4. Observational Hubble Datasets (OHD)

To constrain the cosmological model's parameters, a combination of observational datasets, including Pantheon Supernovae samples, baryon acoustic oscillation (BAO) datasets, and cosmic chronometer (CC) datasets, is utilized.The Pantheon Supernovae samples provide a total of 1048 data points, whereas the BAO and CC datasets contribute 6 and 57 data points, respectively. The emcee Python library is employed, which leverages the Markov Chain Monte Carlo (MCMC) method for Bayesian inference and likelihood estimation.This approach facilitates efficient exploration of the parameter space, yielding reliable constraints on our cosmological model.

Table 1. Constrained values of model parameters and R^2 values.

Datasets	H_0	b	R^2
Pantheon	$67.07^{+1.22}_{-1.22}$	$0.59997^{+0.00016}_{-0.00016}$	0.8062
OHD	$68.01^{+1.57}_{-1.54}$	$0.59996^{+0.00016}_{-0.00016}$	0.8144

A statistical analysis of these cosmological parameters is currently being conducted.The subsequent step involves combining observational Hubble data, specifically $H(z)$ values, to determine the optimal fit for the model parameters b and n. To validate the approach, the model parameters b and n are constrained using observational datasets, which yield the best-fit values of the model parameters.

Dataset have latest 57 data points of $H(z)$ in the red-shift range $0.07 \leq z \leq 2.4$ in which 31 points from Differential Age (DA) method and 26 points from BAO. The best-fit curve of $H(z)$ corresponding to 57 observed data points is obtained using the R^2 - test

$$R^2 = 1 - \frac{\sum_1^{57}[(H_i)_{obs} - (H_i)_{th}]^2}{\sum_1^{57}[(H_i)_{obs} - (H_i)_{mean}]^2}, \tag{40}$$

where $(H_i)_{obs}$ are observed value and $(H_i)_{th}$ are theoretical values obtained from the best fit plot.

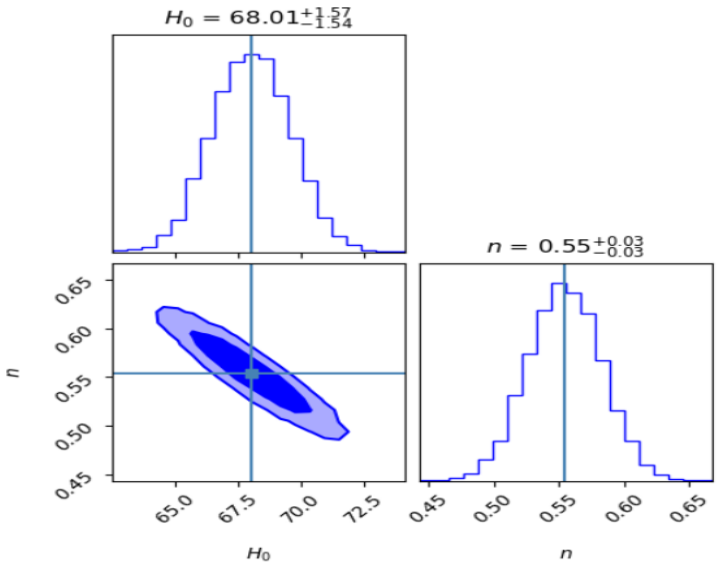

Fig. 1. Contour plot for the Hubble dataset (z).

5. Apparent Magnitude and Luminosity Distance

The expansion of the universe is strongly supported by observations of Type Ia Supernovae (SNe-Ia). Observations of Type Ia supernovae (SNeIa) have consistently supported the expanding universe paradigm. The SNeIa dataset utilized in this study is compiled from various astronomical surveys, including the Panoramic Survey Telescope and Rapid

Response System, the Sloan Digital Sky Survey (SDSS), the Supernovae Legacy Survey (SNLS), and the Hubble Space Telescope (HST) survey [51].

The total flux of the source of light is measured by the luminosity distance is

$$d_L = (1+z)\int_0^z \frac{H_0}{H(z')}dz' \tag{41}$$

To determine best fit values of H_0, the apparent magnitude in terms of d_L is defined as:

$$\tau(z) = M + 5log_{10}d_L - 5log_{10}\left(\frac{H_0}{Mpc}\right) + 25, \tag{42}$$

where, M is constant for all SNeIa

The distance modulus $\mu(z) = \tau - M$ is given by

$$\mu(z) = 5log_{10}d_L - 5log_{10}\left(\frac{H_0}{Mpc}\right) + 25 \tag{43}$$

To obtain the best fit curve of apparent magnitude $\tau(z)$ with the use of the pantheon sample dataset of 1048 points of distance moduli $\mu(z)$ towards the range $0.01 \leq z \leq 2.26$ for various redshifts [52]. From [53] the statistically significant value of M is -19.30.

$$R^2 = 1 - \frac{\sum_1^{1048}[(\mu_i)_{obs} - (\mu_i)_{th}]^2}{\sum_1^{1048}[(\mu_i)_{obs} - (\mu_i)_{mean}]^2} \tag{44}$$

Since $d_L(z)$, $m(z)$, and $\mu(z)$ become undefined at $z = -1$, the parameter space is restricted by setting $z > -1$ and $H_0 > 0$.

Using both the Hubble $H(z)$ data and the Pantheon compilation, the R^2-test is performed to determine the best-fit values for the model parameters α and H_0. Figs. 1 and 2 show the maximum likelihood contours for these parameters, along with their 1σ and 2σ confidence intervals.

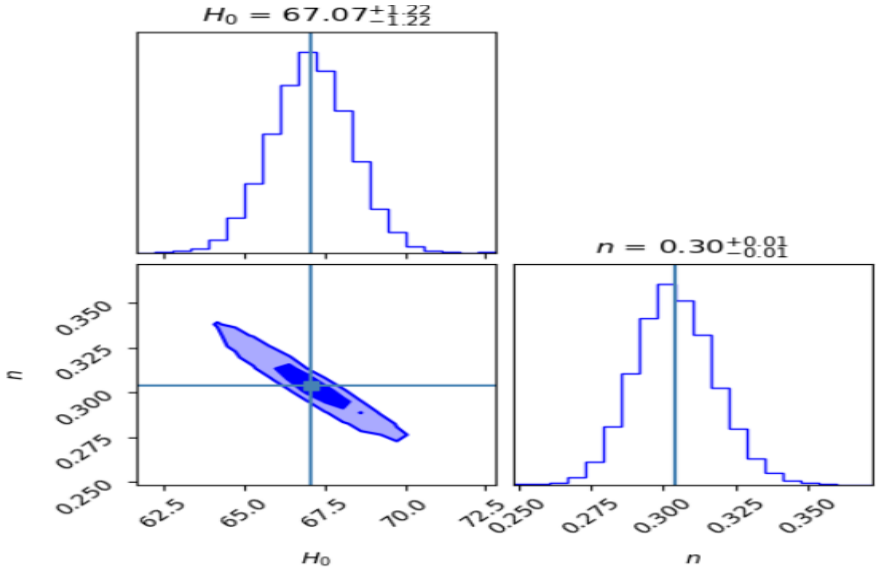

Fig. 2. Contour plot for the Pantheon dataset.

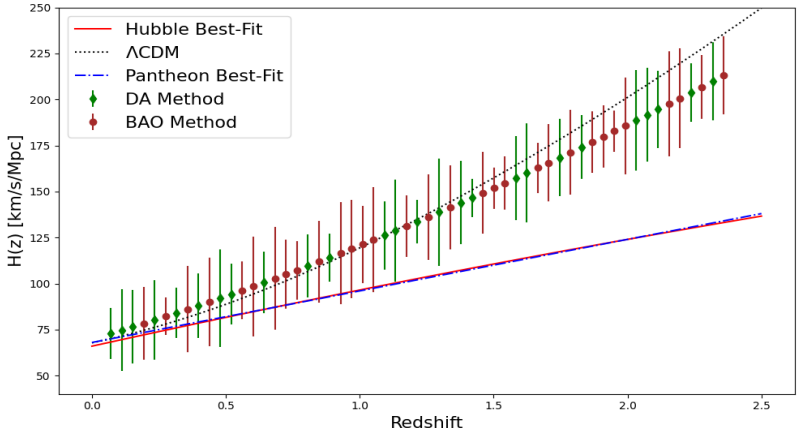

Fig. 3. Error bar plot for 57 Hubble dataset points with best-fit curves.\

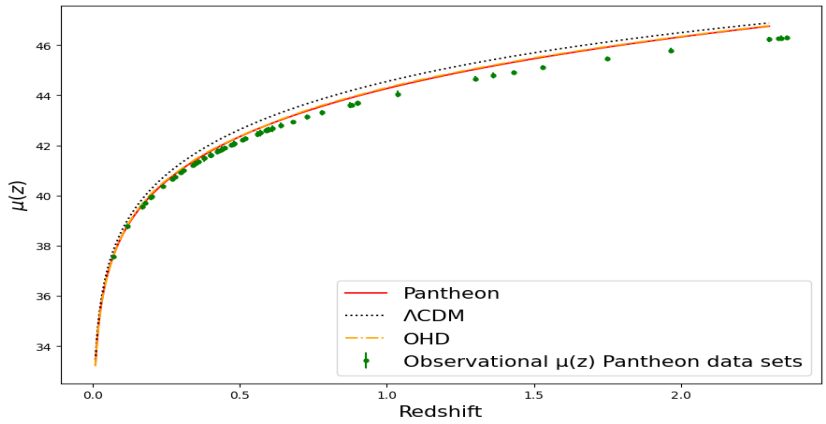

Fig. 4. Error bar plot for 1048 Pantheon dataset points with best-fit curves.

Figs. 3 and 4 display the error bar plots for the 57 data points from the Hubble dataset and the 1048 data points from the Pantheon dataset, using the model parameter values listed in Table 1. Both datasets are compared to the standard ΛCDM model (shown as a dotted black line), with parameters set as $H_0 = 67.8$ km/s/Mpc, $\Omega_{\Lambda_0} = 0.7$, and $\Omega_{m_0} = 0.3$.

6. Cosmographic Parameters and Energy Conditions

To understand the evolution of the universe through different phases, it is essential to analyze key cosmological parameters such as the deceleration parameter (q), pressure (p), density (ρ), and energy conditions.

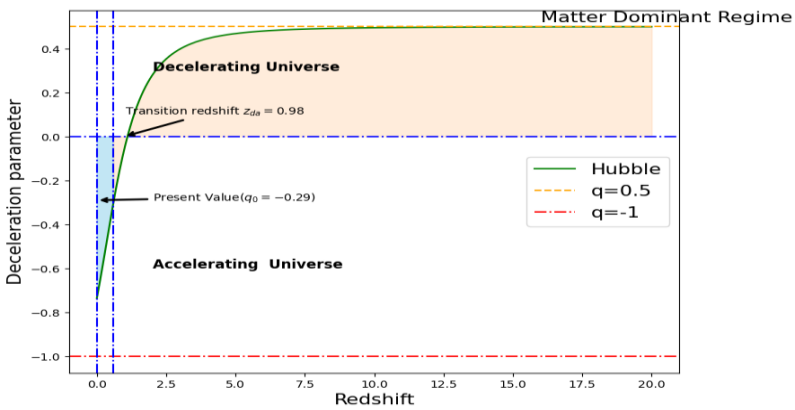

Fig. 5. Evolution of the deceleration parameter with redshift for the Hubble dataset.

From figure, a positive value of q indicates that the universe is decelerating, whereas a negative value signifies accelerated expansion. The point where the universe transitions from deceleration to acceleration is marked by $q = 0$. Numerous studies using Type Ia Supernova (SNe-Ia) observations have shown that the universe was decelerating for redshifts $z > 0.5$, and has been accelerating for $z < 0.5$. In our model, the variation of the deceleration parameter with redshift is illustrated in Figs. 5 and 6, based on both datasets. The parameter values for H_0 and n used in the analysis are listed in Table 1. The redshift values at which the transition from deceleration to acceleration occurs are $z_{da} = 0.59$ for the Hubble dataset and $z_{da} = 0.98$ for the Pantheon dataset.

At present ($z = 0$), the deceleration parameter is $q_0 = -0.25$ for the Hubble dataset and $q_0 = -0.29$ for the Pantheon dataset.

Additionally, for $z > 10$, the deceleration parameter approaches a matter dominated regime ($q \approx 0.5$) in the Hubble dataset, signifying a late-time cosmic evolution.

Pressure (p_x, p_y) and energy density (ρ):

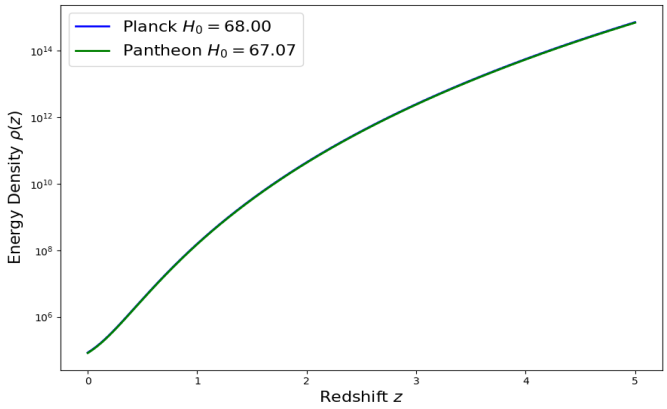

Fig. 6. Evolution of energy density as a function of redshift for the Hubble and Pantheon datasets.

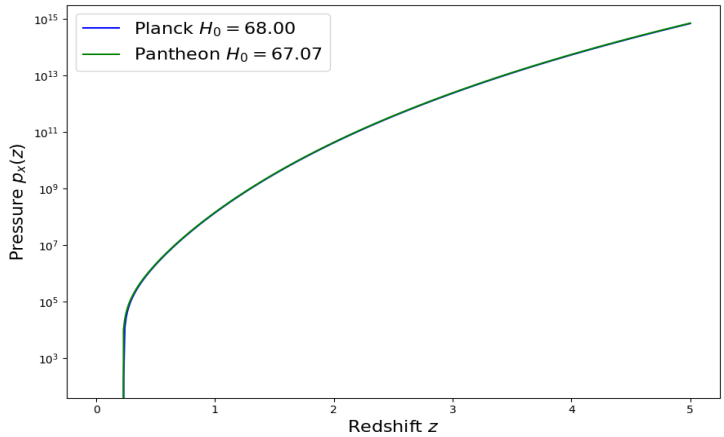

Fig. 7. Evolution of Pressure p_x as a function of redshift for the Hubble and Pantheon datasets.

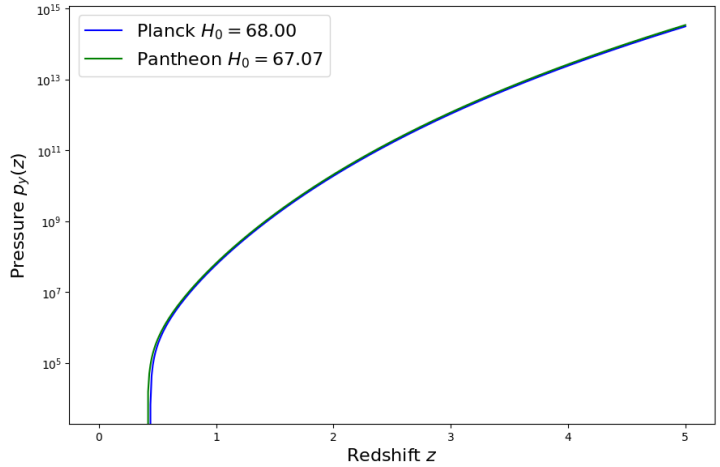

Fig. 8. Evolution of Pressure p_y as a function of redshift for the Hubble and Pantheon datasets.

Eqs. (32) - (34) describe the evolution of x and y component of pressure and energy density in terms of redshift. Figs. 6-8 show the variation of these parameters based on the best-fit values from the Hubble and Pantheon datasets with constant parameter set to $\alpha = 0.5, \eta = n = k = 1, b = 2$.

As shown in Fig. 6, energy density increases with redshift, indicating a higher density in the early universe and a decreasing trend as the universe expands.

Figs. 7 and 8 illustrates that the x and y component of pressure remains negative throughout the cosmic evolution and decreases with redshift. This aligns with the accelerated expansion observed in recent cosmological studies.

Energy conditions are essential concepts in general relativity, providing the foundation for key theorems about the behavior of intense gravitational fields and the structure of the universe. The energy condition for our model are presented in Figs. 9 to 11. These figures

are generated using the best fit values of the Hubble and Pantheon datasets from Table 1 with constant parameters set to $\alpha = 0.5, \eta = n = k = 1, b = 6$.

The four main energy conditions are described as follows:

- Strong Energy Condition (SEC): Requires gravity to be attractive:
  $\rho + 3p \geq 0$.
- Dominant Energy Condition (DEC): Ensures that energy density remains positive and propagates causally:
  $\rho \geq |p|$.
- Weak Energy Condition (WEC): Implies that the measured energy:
  $\rho \geq 0, \rho + p \geq 0$.
- Null Energy Condition (NEC): Represents the most fundamental condition required for WEC and SEC:
  $\rho + p \geq 0$.

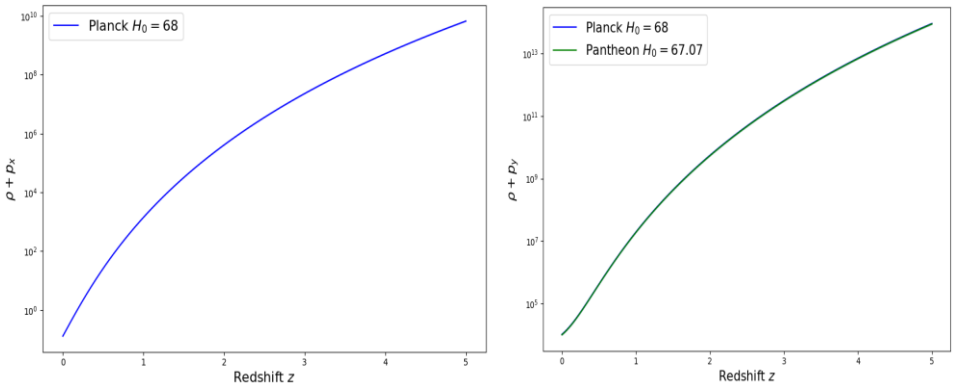

Fig. 9. Evolution of the Weak Energy Condition (WEC) with redshift.

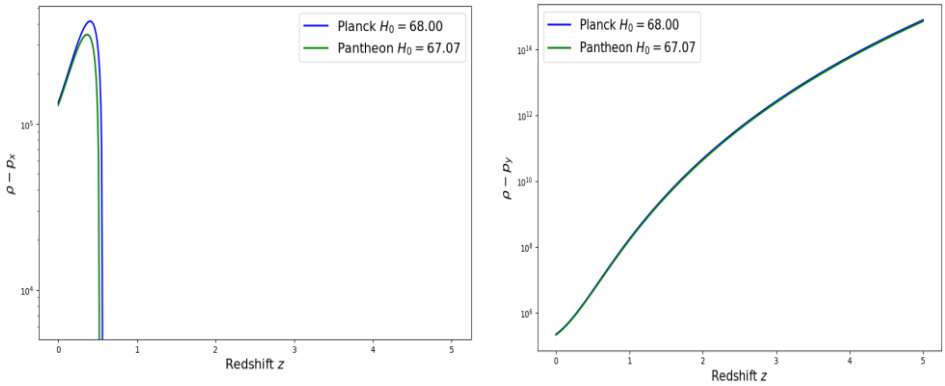

Fig. 10. Evolution of the Dominant Energy Condition (DEC) with redshift.

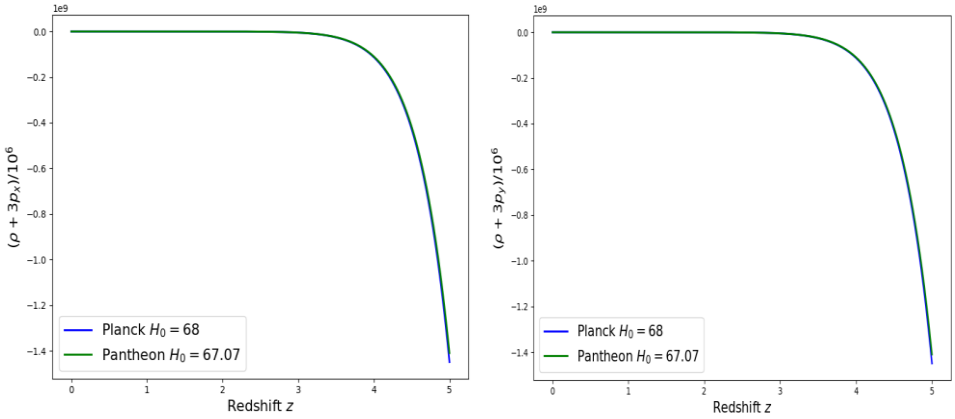

Fig. 11. Strong Energy Condition (SEC) violation with redshift.

The Strong Energy Condition (SEC) is especially important for understanding the present accelerated expansion of the universe. In typical cosmological models, the SEC is anticipated to be violated during periods of cosmic acceleration.

Our model reveals that DEC and WEC are satisfied ensuring that the model remains physically viable. SEC is violated for late-time evolution (see Fig. 11). This aligns with the expectation that SEC must be violated in models that describe an accelerated universe. NEC validation confirms that the WEC is satisfied, reinforcing the physical consistency of our model.

7. Conclusion

This work investigates the cosmological behavior of an anisotropic universe in the framework of $f(G)$ gravity using the LRS Bianchi type-I spacetime. Exact analytical solutions of the field equations were obtained by assuming a proportional relation between the shear scalar and the expansion scalar, along with a time-dependent deceleration parameter. The model parameters were constrained using recent observational datasets from Hubble and Pantheon samples, showing a strong statistical consistency and a good agreement with the observed accelerated expansion of the universe. The positive and monotonically decreasing energy density confirms the physical acceptability of the model throughout cosmic evolution. The directional pressures show a negative trend at late times, indicating a transition from a matter-dominated phase to a dark-energy-dominated phase responsible for acceleration. The analysis of energy conditions demonstrates that the Weak and Dominant Energy Conditions are satisfied, ensuring the stability and realistic nature of the model, while the violation of the Strong Energy Condition supports the occurrence of cosmic acceleration. Overall, the findings establish that the considered $f(G)$ gravity model in an anisotropic Bianchi type-I background provides a viable and observationally

consistent explanation for the late-time accelerated expansion of the universe, while preserving essential physical characteristics of a realistic cosmological model.

References

1. M. De Laurentis and A. J. Lopez-Revelles, Int. J. Geom. Methods Mod. Phys. **11**, ID 1450082 (2014). https://doi.org/10.1142/S0219887814500820
2. H. A. Buchdahl, Mon. Not. R. Astron. Soc. **150**, 1 (1970). https://doi.org/10.1093/mnras/150.1.1
3. K. Atazadeh and F. Darabi, Gen. Relativ. Gravit. **46**, 1664 (2014). https://doi.org/10.1007/s10714-014-1664-8
4. S. Capozziello, M. De Laurentis, and S. D. Odintsov, Mod. Phys. Lett. A **29**, ID 14501648 (2014). https://doi.org/10.1142/S0217732314501648
5. R. Myrzakulov, D. S. Gomez, and A. Tureanu, Gen. Relativ. Gravit. **43**, 1671 (2011). https://doi.org/10.1007/s10714-011-1149-y
6. N. Dadhich, J. Math. Phys. **48**, 331 (2007). https://doi.org/10.1142/9789812770523_0032
7. K. Bamba, A. N. Makarenko, A. N. Myagky, and S. D. Odintsov, Phys. Lett. B **732**, 149 (2014). https://doi.org/10.1016/j.physletb.2014.04.004
8. Z. Kang, Y. Z. Ying, Z. D. Cheng, and Y. R. Hong, Chin. Phys. B **21**, ID 020401 (2012). https://doi.org/10.1088/1674-1056/21/2/020401
9. A. Y. Shaikh, S. V. Gore, and S. D. Katore, New Astron. **80**, ID 101420 (2020). https://doi.org/10.1016/j.newast.2020.101420
10. K. Bamba, S. Capozziello, S. I. Nojiri, and S. D. Odintsov, Astrophys. Space Sci. **342**, 155 (2012). https://doi.org/10.1007/s10509-012-1181-8
11. S. I. Nojiri and S. D. Odintsov, Phys. Rep. **505**, 59 (2011). https://doi.org/10.1016/j.physrep.2011.04.001
12. G. Hinshaw, D. Larson, E. Komatsu, D. N. Spergel, C. Bennett *et al.*, Astrophys. J. Suppl. Ser. **208**, 19 (2013). https://doi.org/10.1088/0067-0049/208/2/19
13. P. Khade, Jordan J. Phys. **16**, 51 (2023). https://doi.org/10.47011/16.1.5
14. M. Jamil, D. Momeni, M. Raza, and R. Myrzakulov, Eur. Phys. J. C **72**, 1999 (2012). https://doi.org/10.1140/epjc/s10052-012-1999-9
15. G. Steigman, R. C. Santos, and J. A. S. Lima, J. Cosmol. Astropart. Phys. **06**, ID 033 (2009). https://doi.org/10.1088/1475-7516/2009/06/033
16. V. Fayaz, H. Hossienkhani, and A. Aghamohammadi, Astrophys. Space Sci. **357**, 136 (2015). https://doi.org/10.1007/s10509-015-2367-7
17. B. Li, J. D. Barrow, and D. F. Mota, Phys. Rev. D **76**, ID 044027 (2007).
18. S. Nojiri, S. D. Odintsov, and M. Sasaki, Phys. Rev. D **71**, ID 123509 (2005). ttps://doi.org/10.1103/PhysRevD.71.123509
19. S. C. Davis, arXiv:0709.4453.
20. A. De Felice and S. Tsujikawa, Phys. Rev. D **80**, ID 063516 (2009). https://doi.org/10.1103/PhysRevD.80.063516
21. S. H. Shekh, A. Husain, H. Chaudhary, S. W. Samdurkar, and N. Myrzakulov, Mod. Phys. Lett. A **39**, 2450099 (2024). https://doi.org/10.1142/S0217732324500998
22. S. Nojiri, S. D. Odintsov, and O. G. Gorbunova, J. Phys. A **39**, 6627 (2006). https://doi.org/10.1088/0305-4470/39/21/S62
23. G. Cognola, E. Elizalde, S. Nojiri, S. D. Odintsov, and S. Zerbini, Phys. Rev. D **73**, ID 084007 (2006). https://doi.org/10.1103/PhysRevD.73.084007
24. S. Nojiri, S. D. Odintsov, and M. Sami, Phys. Rev. D **74**, ID 046004 (2006). https://doi.org/10.1103/PhysRevD.74.046004
25. S.-Y. Zhou, E. J. Copeland, and P. M. Saffin, J. Cosmol. Astropart. Phys. **07**, ID 009 (2009). https://doi.org/10.1088/1475-7516/2009/07/009

26. N. Goheer, R. Goswami, K. S. Peter, P. Dunsby, and K. Ananda, Phys. Rev. D **79**, ID 121301 (2009). https://doi.org/10.1103/PhysRevD.79.121301
27. K. Uddin, J. E. Lidsey, and R. Tavakol, Gen. Relativ. Gravit. **41**, 2725 (2009). https://doi.org/10.1007/s10714-009-0803-0
28. C. G. Boehmer and F. S. N. Lobo, Phys. Rev. D **79**, ID 067504 (2009).
29. M. Alimohammadi and A. Ghalee, Phys. Rev. D **79**, ID 063006 (2009). https://doi.org/10.1103/PhysRevD.79.063006
30. A. De Felice and S. Tsujikawa, Phys. Lett. B **675**, 1 (2009). https://doi.org/10.1016/j.physletb.2009.03.060
31. G. Cognola, E. Elizalde, S. Nojiri, S. D. Odintsov, and S. Zerbini, Phys. Rev. D **75**, ID 086002 (2007). https://doi.org/10.1103/PhysRevD.75.086002
32. M. Gurses, *Gen.* Relativ. Gravit. **40**, 1825 (2008). https://doi.org/10.1007/s10714-007-0579-z
33. S. Nojiri, S. D. Odintsov, and P. V. Tretyakov, Phys. Lett. B **651**, 224 (2007). https://doi.org/10.1016/j.physletb.2007.06.029
34. K. Bamba, S. D. Odintsov, L. Sebastiani, and S. Zerbini, Eur. Phys. J. C **67**, 295 (2010). https://doi.org/10.1140/epjc/s10052-010-1292-8
35. S. Capozziello, M. De Laurentis, S. Nojiri, and S. D. Odintsov, Phys. Rev. D **79**, ID 124007 (2009). https://doi.org/10.1103/PhysRevD.79.124007
36. S. Nojiri and S. D. Odintsov, Phys. Rev. D **68**, ID 123512 (2003). https://doi.org/10.1103/PhysRevD.68.123512
37. K. Bamba, S. Nojiri, and S. D. Odintsov, J. Cosmol. Astropart. Phys. **10**, ID 045 (2008). https://doi.org/10.1088/1475-7516/2008/10/045
38. E. Elizalde, R. Myrzakulov, V. V. Obukhov, and D. Saez-Gomez, Class. Quantum Grav. **27**, ID 095007 (2010). https://doi.org/10.1088/0264-9381/27/9/095007
39. V. J. Dagwal and D. D. Pawar, arXiv:1704.07107.
40. D. D. Pawar and Y. Solanke, Turk. J. Phys. **39**, 54 (2015). https://doi.org/10.3906/fiz-1404-1
41. D. D. Pawar, Y. S. Solanke, and S. P. Shahare, Bulgarian J. Phys. **41**, 60 (2014).
42. D. D. Pawar, N. G. Ghungarwar, S. Muhammad, and E. Zotos, Astron. Comput. **51**, ID 100924 (2025). https://doi.org/10.1016/j.ascom.2024.100924
43. D. D. Pawar, P. S. Gaikwad, S. Muhammad, and E. E. Zotos, Astron. Comput. **48**, ID 100863 (2024). https://doi.org/10.1016/j.ascom.2024.100863
44. S. Samdurkar, R. Pathekar, R. Tambatkar, and S. Bawnerkar, J. Sci. Res. **17**, 367 (2025). https://doi.org/10.3329/jsr.v17i2.74136
45. K. N. Pawar and M. D. Netnaskar, J. Sci. Res. **17**, 407 (2025). ttps://doi.org/10.3329/jsr.v17i2.75357
46. R. K. Tiwari, A. Beesham, and B. K. Shukla, Int. J. Geom. Methods Mod. Phys. **15**, ID 1850115 (2018). https://doi.org/10.1142/S0219887818501153
47. R. K. Tiwari and D. Sofuoglu, Int. J. Geom. Methods Mod. Phys. **17**, ID 2030003 (2021). https://doi.org/10.1142/S0219887820300032
48. A. G. Riess, A. V. Fillippenko, P. Challis, A. Clocchiatti *et al.*, Astron. J. **116**, 1009 (1998). https://doi.org/10.1086/300499
49. S. Perlmutter, G. Aldering, G. Goldhaber, R. A. Knop, P. Nugent *et al.*, Astrophys. J. **517**, 565 (1999). https://doi.org/10.1086/307221
50. D. N. Spergel, M. Bolte, and W. Freedman, Proc. Natl. Acad. Sci. U.S.A. **94**, 6579 (1997). https://doi.org/10.1073/pnas.94.13.6579
51. D. M. Scolnic, D. O. Jones, A. Rest, Y. C. Pan, R. Chornock *et al.*, Astrophys. J. **859**, 101 (2018). https://doi.org/10.3847/1538-4357/aab9bb
52. V. G. Mete and P. S. Dudhe, J. Sci. Res. **17**, 141 (2025). https://doi.org/10.3329/jsr.v17i1.74327
53. P. Kumawat, R. Goyal, and S. Choudhary, J. Sci. Res. **16**, 695 (2024). https://doi.org/10.3329/jsr.v16i3.70809